Journal of Quantitative Spectroscopy & Radiative Transfer 238 (2019) 106547

Contents lists available at ScienceDirect

Journal of Quantitative Spectroscopy & Radiative Transfer

journal homepage: www.elsevier.com/locate/jqsrt

Ozone isotopologue measurements from the Atmospheric Chemistry Experiment (ACE)

Anton M. Fernando[a,*], Peter F. Bernath[a,b], Christopher D. Boone[c]

[a] Old Dominion University, Department of Physics, Norfolk,VA 23529, USA
[b] Old Dominion University, Department of Chemistry and Biochemistry, Norfolk, VA 23529, USA
[c] Department of Chemistry, University of Waterloo, Waterloo, Ontario, Canada

ARTICLE INFO

Article history:
Received 16 February 2019
Revised 8 June 2019
Accepted 20 June 2019
Available online 22 June 2019

Keywords:
Ozone isotopologues
Fourier transform spectroscopy
Satellite remote sensing

ABSTRACT

Near global ozone isotopologue distributions have been determined from infrared solar occultation measurements of the Atmospheric Chemistry Experiment (ACE) satellite mission. ACE measurements are made with a high resolution Fourier transform spectrometer. Annual and seasonal latitudinal fractionation (δ value) distributions of the ozone isotopologues $^{16}O^{16}O^{18}O$, $^{16}O^{18}O^{16}O$ and $^{16}O^{17}O^{16}O$ were obtained. Asymmetric ozone ($^{16}O^{16}O^{18}O$) shows higher fractionation compared to symmetric ozone ($^{16}O^{18}O^{16}O$). The maximum ozone fractionation occurs in the tropical stratosphere as expected from the contribution of photolysis to the enrichment of heavy isotopologues. An enhancement of the heavy ozone isotopologues is also seen in the upper stratosphere of the Antarctic polar vortex.

1. Introduction

Isotopically-substituted ozone is highly enriched in the Earth's stratosphere compared to the normal ozone isotopic abundances. As this isotopic signature can be transfered to other trace gases such as CO_2, CO and N_2O, it can be used to obtain information on atmospheric transport and chemical reactions. In 1980, Cicerone and McCrumb [1] suggested that because the photodissociation rate of $^{16}O^{18}O$ is significantly greater than that of $^{16}O^{16}O$, an enrichment of ozone should be expected above 40 km in the Earth's atmosphere. In 1981, Mauersberger [2] found, using balloon-based mass spectrometric measurements, that the stratosphere is relatively enriched with $^{16}O^{18}O^{16}O$ and $^{16}O^{16}O^{18}O$. Mass spectrometric observations made by Mauersberger et al. [3] in the midstratosphere of $^{50}O_3$ ($^{50}O_3$ represents the isotopomers $^{16}O^{16}O^{18}O$ and $^{16}O^{18}O^{16}O$ regardless of the symmetry) showed 7–9% enrichment and $^{49}O_3$ ($^{49}O_3$ represents the isotopologues $^{16}O^{16}O^{17}O$ and $^{16}O^{17}O^{16}O$ regardless of the symmetry) of 7–11%. Mass spectrometric data of Krankowsky et al. [4] showed that the $^{50}O_3$ enrichment at 22–33 km is 7–11% and the $^{49}O_3$ enrichment is slightly lower relative to $^{50}O_3$. More recent balloon measurements by Krankowsky et al. [5] have determined the latitude and altitude dependence of heavy ozone enrichment. Far-infrared emission spectra [6] showed 12.3% enrichment for $^{50}O_3$ and 10.7% for $^{49}O_3$. Similarly, solar occultation spectroscopy by the ATMOS instrument in orbit [7] also confirmed a significant isotopic enrichment in the stratosphere. $^{16}O^{16}O^{18}O$ and $^{16}O^{18}O^{16}O$ measurements were obtained from MIPAS (Michelson Interferometer for Passive Atmospheric Sounding) [8]. The symmetric isotopomer $^{16}O^{16}O^{18}O$ shows ~8% enrichment with an increasing vertical profile up to 33 km and with decreasing values at higher altitudes and the asymmetric isotopomer $^{16}O^{18}O^{16}O$ shows values around 3% [8]. This enrichment for heavy isotopes is found in laboratory measurements as well, supporting the atmospheric observations [9–11].

The main process responsible for ozone fractionation in the stratosphere is ozone formation by the three body recombination reaction (XY + Z + M → XYZ + M; X, Y, Z represent different oxygen isotopes). In this recombination process a vibrationally excited ozone complex is formed and is stabilized to form normal ozone (XY + Z ⇌ XYZ* → XYZ). The ozone complex can also dissociate by two fragmentation channels (X + YZ ← XYZ* → XY + Z). The exchange reaction (X + YZ ⇌ XY + Z) also plays a significant role in ozone fractionation [12,13]. Isotopic fractionation is explained by the different reaction rates for the recombination reaction and the ozone exchange reaction with different atomic isotopes and molecular isotopologues and isotopomers [12,14,15]. An isotopologue is any isotopically substituted molecule and an isotopomer is an isotopic isomer such as $^{16}O^{16}O^{18}O$ and $^{16}O^{18}O^{16}O$ where both species are isotopologues.

The other process that contributes to ozone fractionation is photolysis of O_3. O atoms are generated by O_3 photolysis and react with stratospheric O_2 to re-form ozone. Ozone is photolized to produce singlet and triplet oxygen atoms ($O_3 + h\nu \rightarrow O(^1D) +$

* Corresponding author.
E-mail address: afern018@odu.edu (A.M. Fernando).

https://doi.org/10.1016/j.jqsrt.2019.06.026
0022-4073/

$O_2(^1\Delta_g)$ and $O_3 + h\nu \rightarrow O(^3P) + O_2(^3\Sigma_g^-)$). $O(^1D)$ atoms produced by this photolysis reaction can be quenched by N_2 and O_2 to produce more $O(^3P)$ atoms which recombine with O_2 to produce O_3. Odd oxygen (O and O_3) react to re-form molecular oxygen ($O + O_3 \rightarrow 2O_2$) to keep the ozone budget balanced. Since odd oxygen cycling is faster than the sink and source reactions, it limits the ozone fractionation significantly [13].

Ozone formation contributes more to isotopic enrichment than photolysis and the contribution of photolysis was not recognized as significant until recently [16]. If the isotopic fractionation is proportional to the mass difference from the parent isotopologue, then it is called mass dependent fractionation (e.g., the fractionation of $^{16}O^{18}O^{16}O$ should be about twice as large as that of $^{16}O^{17}O^{16}O$). The ozone enrichment observed in the stratosphere is mass independent because the enrichments for ^{17}O are similar to those for ^{18}O.

Chakraborty and Bhattacharya [17] showed through laboratory experiments that the photolysis process that contributes to ozone fractionation is mass independent in the UV. Cole and Boering [18] demonstrated by detailed kinetic modeling that the experiments carried out by Chakraborty and Bhattacharya [17] neglected new ozone formation during their experiments and in fact ozone photolysis is a mass dependent process in both UV and visible regions. Miller et al. [19] and Liang et al. [20] showed using photochemical model calculations and Ndengué et al. [21] with *ab initio* photodissociation cross sections that ozone photolysis is mass dependent. Früchtl et al. [22] measured the fractionation in the visible region and confirmed the mass dependence, but noted that their values disagreed with the semi-analytical model of Liang et al. [20]. Wavelength and altitude dependence of the photolysis process is also shown in the studies of Liang et al. [20], Früchtl et al. [22], 23] and Miller et al. [19].

2. Observations and retrievals

The ACE (Atmospheric Chemistry Experiment) satellite (also known as SCISAT) has been in orbit since August, 2003 [24]. The ACE Fourier Transform Spectrometer (FTS) measures a large number of molecules and isotopologues in the Earth's atmosphere from a low Earth circular orbit (altitude 650 km, inclination 74°). In addition to volume mixing ratio (VMR) profiles of atmospheric trace gases, ACE-FTS provides altitude information for temperature, pressure and atmospheric extinction profiles. ACE-FTS records infrared spectra using the solar occultation technique during sunset and sunrise in the limb geometry. ACE-FTS operates in the 750–4400 cm^{-1} spectral region with a resolution of 0.02 cm^{-1}. Ozone and its isotopologue VMR profiles ($^{16}O^{16}O^{16}O$, $^{16}O^{16}O^{18}O$, $^{16}O^{18}O^{16}O$, $^{16}O^{17}O^{16}O$) are provided on a vertical grid of 1 km from about 5 km (or the cloud tops) up to ~50 km (for the minor isotopologues) covering latitudes 85°N to 85°S [24]. For this work version 3.5/3.6 of ACE-FTS processing is used for 2014–2018 and the ozone microwindows used are provided as supplementary data. Version 3.5/3.6 uses spectroscopic line parameters for ozone from the HITRAN 2004 database [25].

2.1. Fractionation process

Isotopic fractionation is defined as:

$$\delta(\%) = 100\left(\frac{R}{R_0} - 1\right) \quad (1)$$

in which $R = [O_3]_{isotope}/[O_3]$ is the observed isotopic ratio. The convention is that the VMR of the most abundant isotopologue should be in the denominator and the VMR of the less abundant isotopologue in the numerator (R_0 is the reference ratio). For this study, VSMOW (Vienna Standard Mean Ocean Water) is used with $R_0(^{18}O) = 0.00200520$ and $R_0(^{17}O) = 0.000373$ [27]. These reference ratios are only given for atomic oxygen. The likelihood of randomly finding non-symmetric ozone (QOO) in a sample is twice as large as the symmetric ozone (OQO) (with heavy oxygen atom denoted by Q). Therefore the reference VMRs were multiplied by 2 to obtain δ values for non-symmetric isotopologues.

2.2. Data set

There are ozone isotopologue measurements available in the literature for comparison with ACE-FTS values. We used data from the space-based solar absorption spectra recorded by the ATMOS (Atmospheric Trace Molecule Spectroscopy Experiment) Fourier transform spectrometer [7]; data from the balloon-borne solar absorption spectra by the MkIV FTIR (Fourier Transform Infrared) spectrometer [16]; data from mass spectrometer measurements of samples collected with high altitude balloons [5]; data from the Michelson Interferometer for Passive Atmospheric Sounding (MIPAS) [8]; data from the balloon-borne thermal emission spectra by the FIRS-2 Fourier transform spectrometer [6] and MIPAS-Balloon measurements [26] for the validation of ACE-FTS data. The altitude profiles of δ values of $^{50}O_3$ derived from these datasets for 5 latitude bins (polar, mid-latitude and tropics) that are provided in Fig. 3 of the journal paper Jonkheid et al. [8] were used to compare with ACE-FTS data. The altitude profiles of δ values of $^{16}O^{16}O^{18}O$ and δ $^{16}O^{18}O^{16}O$ derived from the MIPAS-Balloon data were extracted from Fig. 4 in the journal paper by Piccolo et al. [26] and the MkIV FTIR data were extracted from Fig. 1 in the journal paper of Haverd et al. [16].

The ATMOS data were derived from the missions Spacelab-3 (April-May 1985), Atlas-1 (March 1992), Atlas-2 (April 1993) and Atlas-3 (November 1994) [7,8]. The FIRS-2 data were obtained from seven balloon flights launched from Fort Sumner (35°N), Daggett (45°N) and Fort Wainwright (65°N) between 1989 and 1997. The mass spectrometer data were taken from 11 balloon flights launched from Kiruna (68°N), Aire sur l'Adour (43.7°N), and Teresina (5°S) between 1998 and 2005 [6,8]. The MkIV FTIR data were obtained from seven balloon flights launched from Fort Sumner (35°N), Esrange (68°N) and Fort Wainwright (65°N) between 1997 and 2003 [8,16]. The measurements from MIPAS-Balloon (balloon-borne version of the MIPAS satellite instrument) were recorded in Aire sur l'Adour, France (43.7°N) on 24 September 2002 and in Kiruna, Sweden (67.5°N) on 20/21 March 2003 [26].

3. Results and discussion

3.1. Analysis

The ACE-FTS provides data for ozone isotopologues from 6.5 km to 49.5 km (but the analysis is restricted to the altitudes 20.5-40.5 km due to the high statistical errors outside the range selected). Initially large negative and positive values (VMR values greater than about 100 ppm and less than about 0.1 ppm) were discarded from isotopologue profiles and δ values were calculated. The calculated δ values were put into 10° latitude bins for each altitude level and values that were more than two standard deviations from the bin average and large positive and negative values were discarded. Then the quarterly mission averages for Dec-Feb (DJF), Mar–May (MAM), Jun–Aug (JJA), Sep–Nov (SON) and the mission average latitudinal distributions of δ values were obtained (Figs. 1–3) for each isotopologue. One standard deviation error bars are also displayed (e.g., Fig. 4).

The mission average (2004-2018) latitudinal distribution of $^{16}O^{16}O^{18}O$ shows fractionations ~20% between the altitudes 21.5–26.5 km, ~15% between the altitudes 27.5–35.5 km and ~12% be-

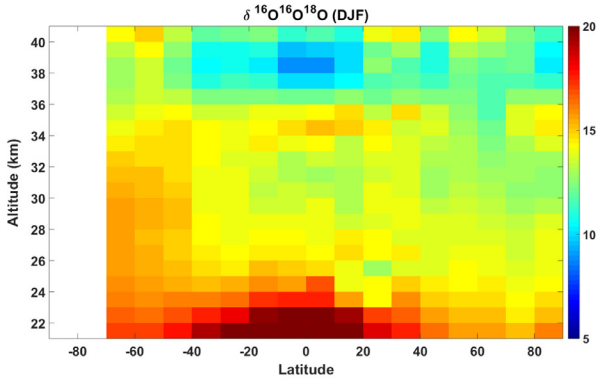

(a) δ $^{16}O^{16}O^{18}O$ % DJF

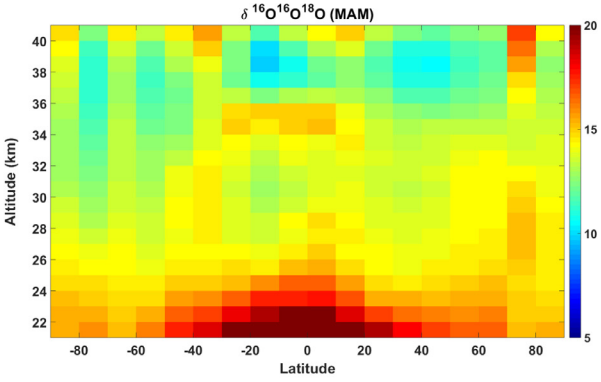

(b) δ $^{16}O^{16}O^{18}O$ % MAM

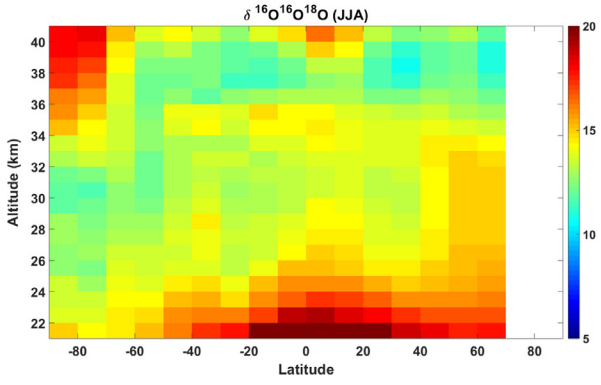

(c) δ $^{16}O^{16}O^{18}O$ % JJA

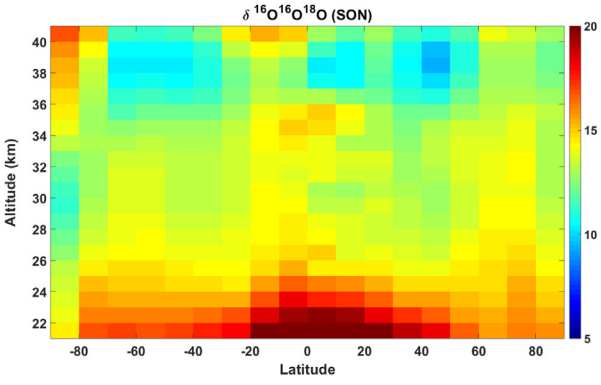

(d) δ $^{16}O^{16}O^{18}O$ % SON

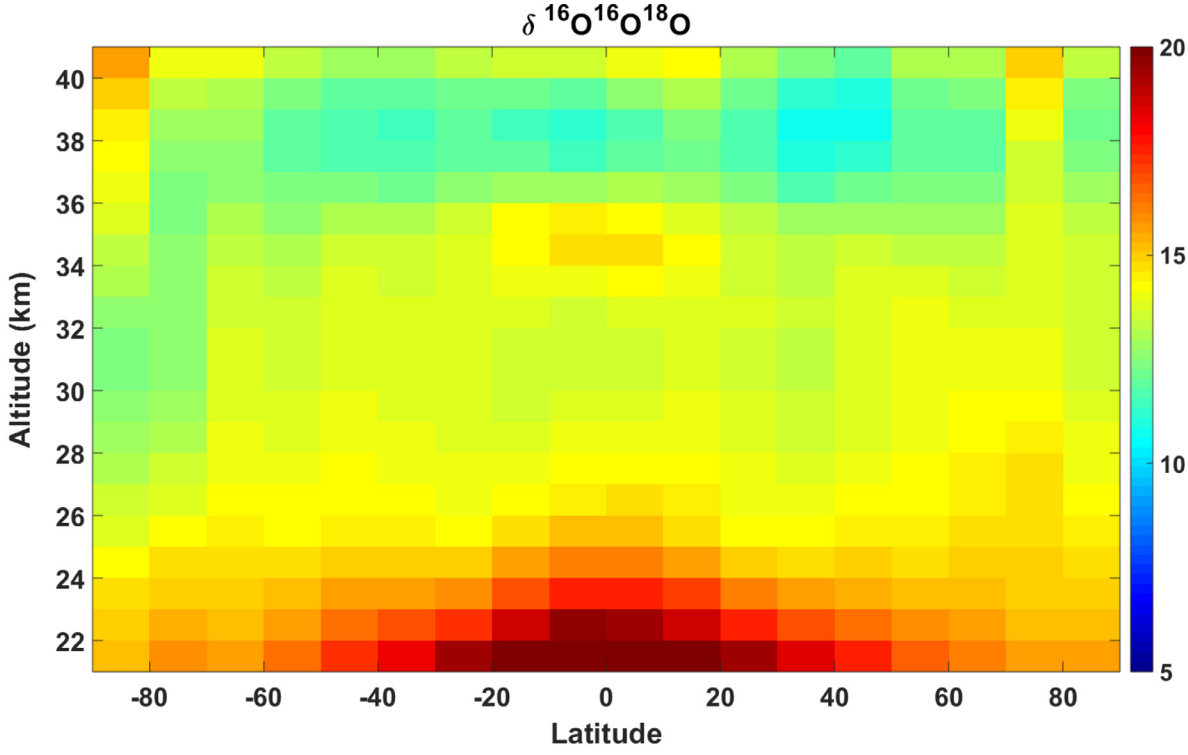

(e) δ $^{16}O^{16}O^{18}O$ % mission average

Fig. 1. δ $^{16}O^{16}O^{18}O$ %

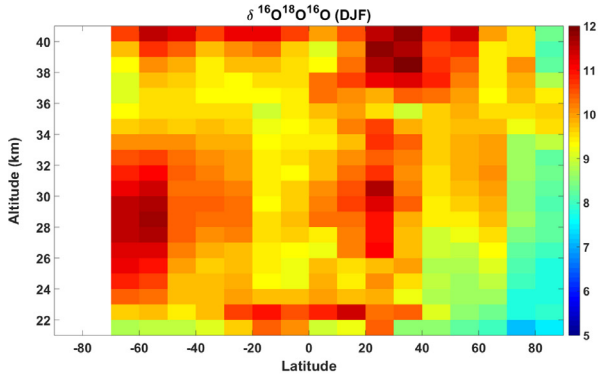

(a) δ $^{16}O^{18}O^{16}O$ % DJF

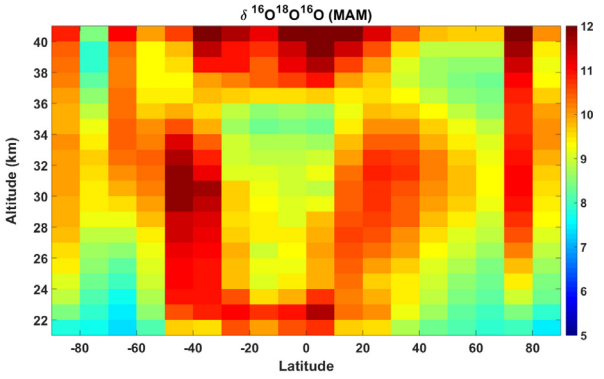

(b) δ $^{16}O^{18}O^{16}O$ % MAM

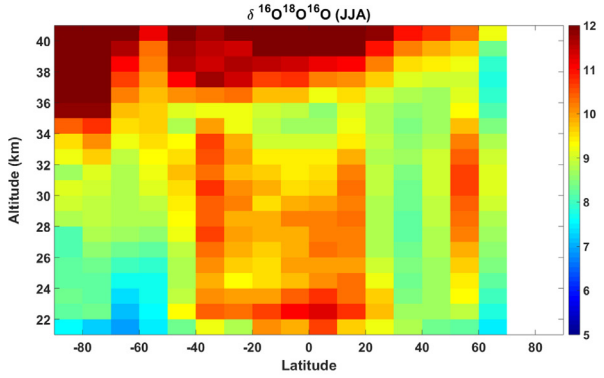

(c) δ $^{16}O^{18}O^{16}O$ % JJA

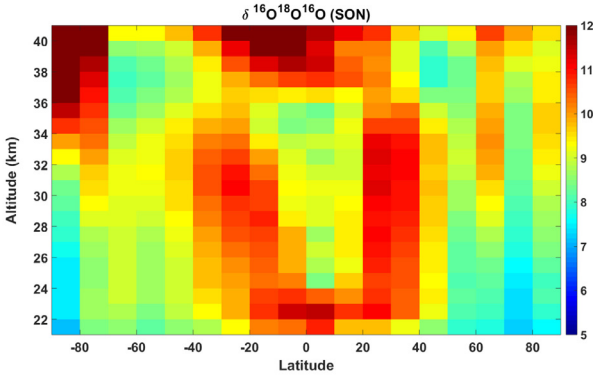

(d) δ $^{16}O^{18}O^{16}O$ % SON

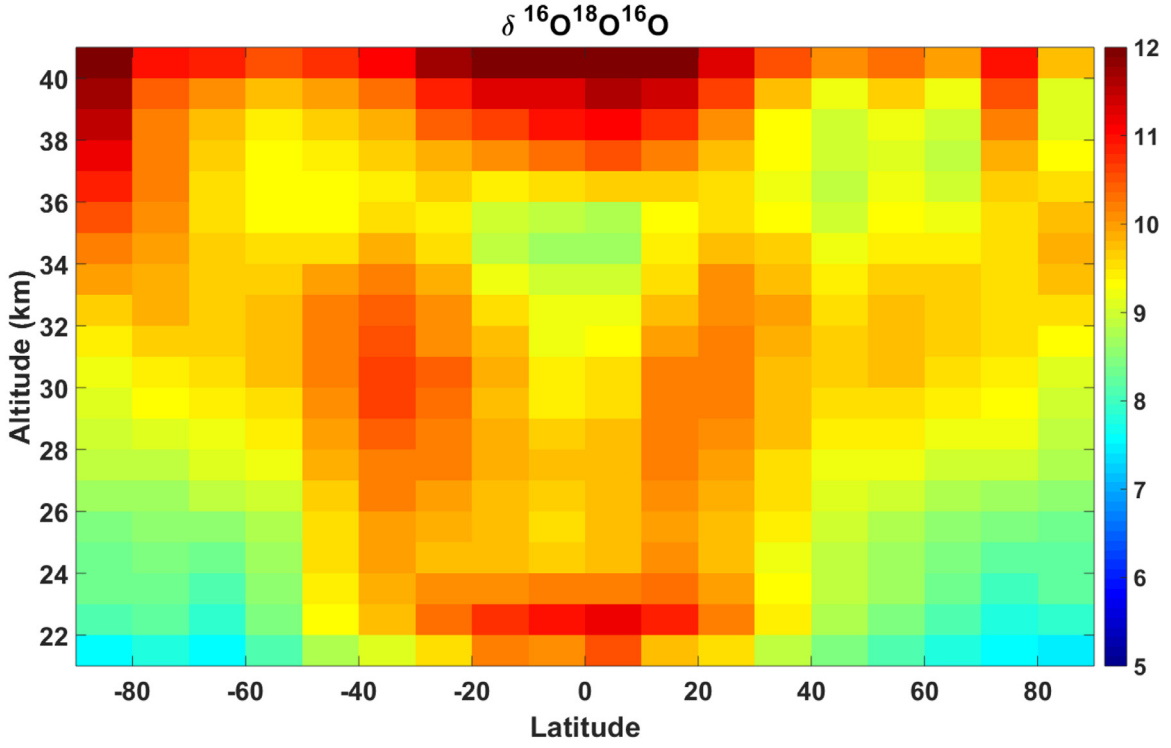

(e) δ $^{16}O^{18}O^{16}O$ mission average %

Fig. 2. δ $^{16}O^{18}O^{16}O$ %

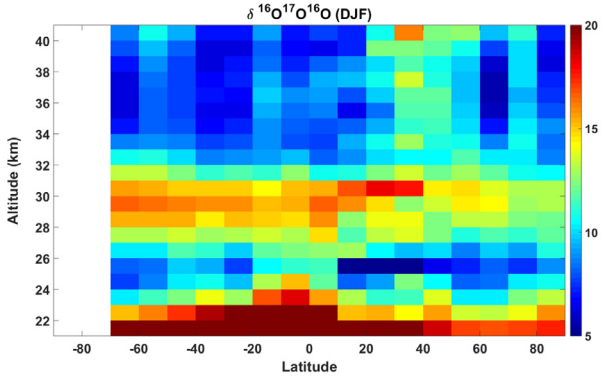

(a) $\delta\ ^{16}O^{17}O^{16}O$ % DJF

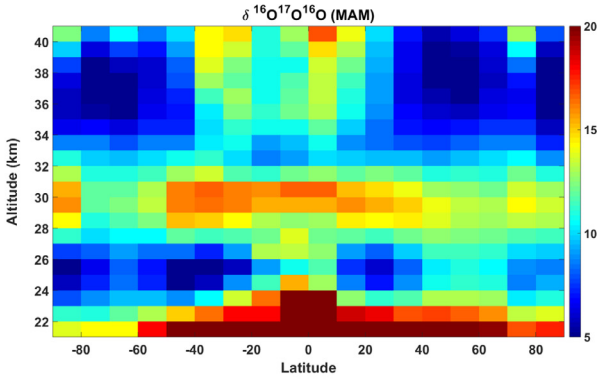

(b) $\delta\ ^{16}O^{17}O^{16}O$ % MAM

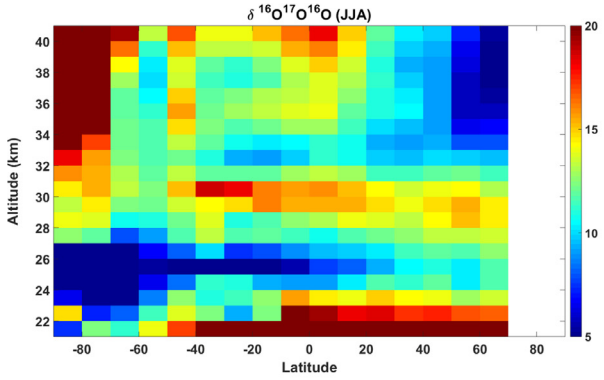

(c) $\delta\ ^{16}O^{17}O^{16}O$ % JJA

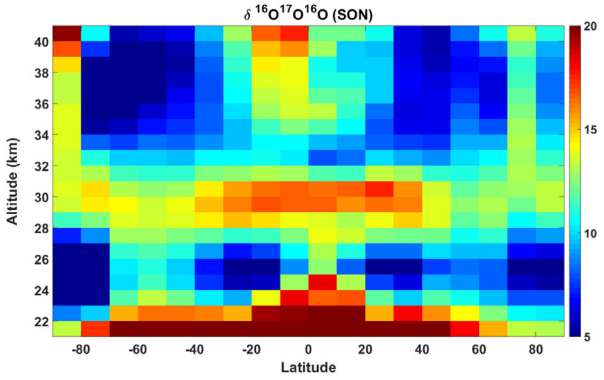

(d) $\delta\ ^{16}O^{17}O^{16}O$ % SON

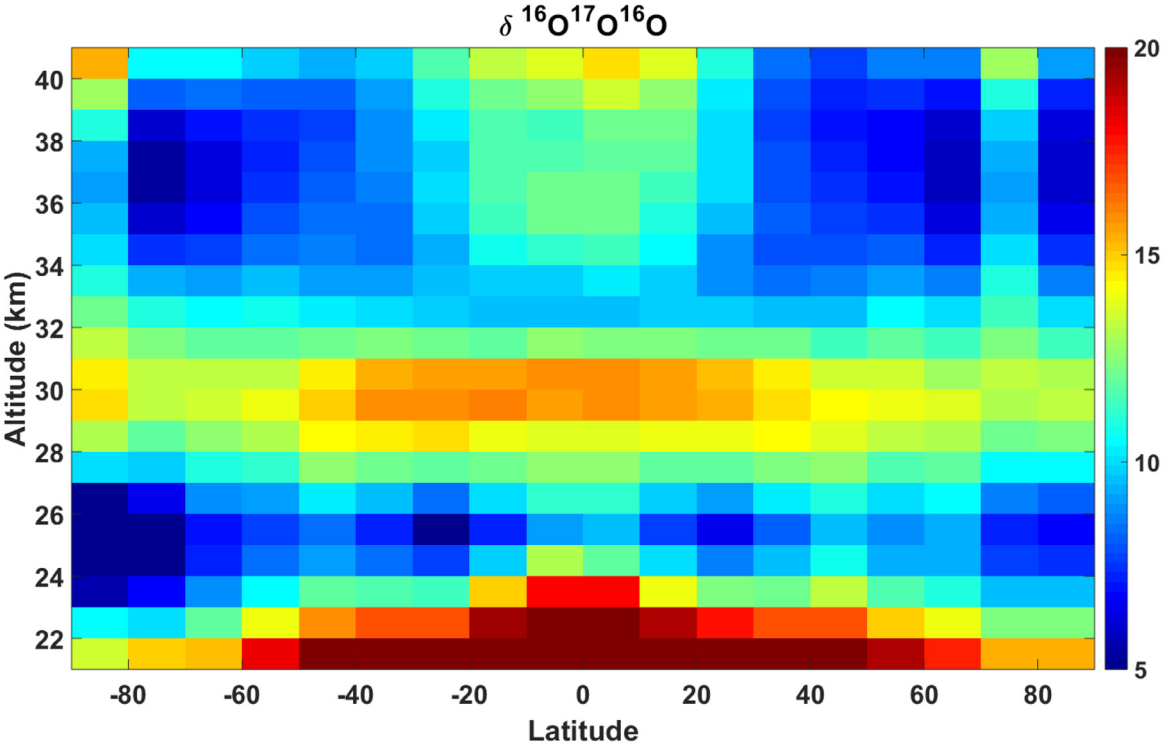

(e) $\delta\ ^{16}O^{17}O^{16}O$ % mission average

Fig. 3. $\delta\ ^{16}O^{17}O^{16}O$ %

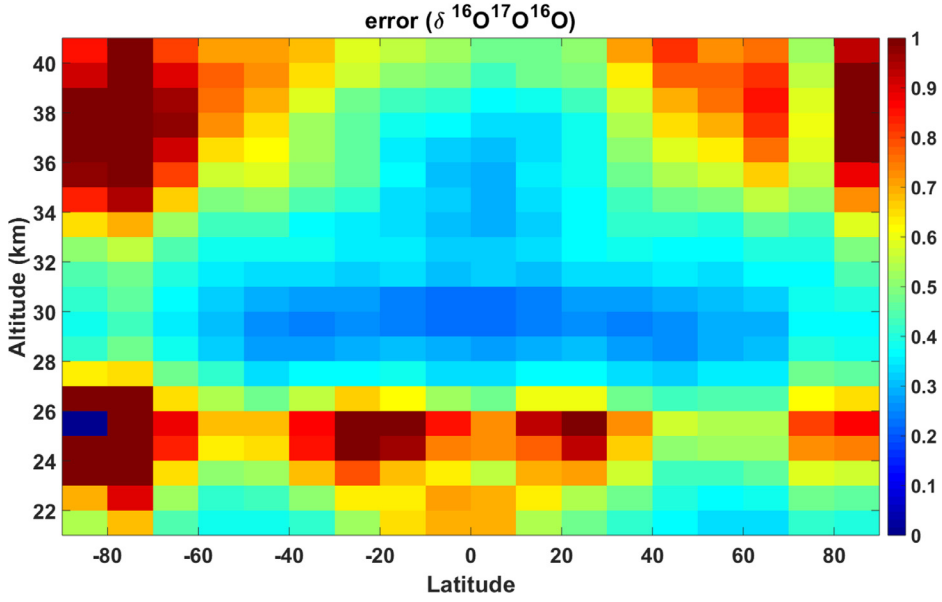

Fig. 4. Standard deviation of δ $^{16}O^{17}O^{16}O$ % altitude-latitude bins

tween the altitudes 36.5–40.5 km in the latitude region 45°S–45°N. The polar region in the Southern Hemisphere (70°S–90°S) shows less fractionation (∼12%) compared to the Northern Hemisphere (∼15%) (70°N–90°N). The seasonal latitudinal distributions of $^{16}O^{16}O^{18}O$ show that there is higher fractionation in the polar regions during summer, JJA in the Northern Hemisphere and DJF in the Southern Hemisphere. These enhancements in the tropics and in the summer at high latitudes are consistent with the contribution of photolysis to fractionation. The δ value standard deviations of the altitude-latitude bins of the mission average latitudinal distribution of the isotopologue $^{16}O^{16}O^{18}O$ are around ∼0.15.

The δ values mission average latitudinal distribution of the isotopologue $^{16}O^{18}O^{16}O$ shows high fractionations 10–12% between the altitudes 21.5–26.5 km and in the latitude region 45°S–45°N and smaller fractionations (8–9%) in the regions 50°–90°S,N and between the altitudes 21.5–26.5 km. Above 30.5 km, fractionations start to increase to 10–11% in the regions 50°–90°S,N. Similar to $^{16}O^{16}O^{18}O$ the $^{16}O^{16}O^{18}O$ mission average latitudinal distribution also shows higher fractionations in the Northern Hemisphere during JJA compared to Southern Hemisphere and in Southern Hemisphere compared to Northern Hemisphere during DJF when more sunlight is available. The effect of photolysis is also evident in the enhanced fractionation for $^{16}O^{18}O^{16}O$ at high altitudes (above 35 km) in the tropics. Ndengué et al. [21] predict that $^{16}O^{18}O^{16}O$ is preferentially fractionated by ozone photolysis in the Hartley bands at this altitude. The absolute standard deviations of the altitude-latitude bins of the mission average latitudinal distribution of the isotopologue $^{16}O^{18}O^{16}O$ are ∼0.2.

The mission average latitudinal distributions of the isotopologues $^{16}O^{18}O^{16}O$ and $^{16}O^{16}O^{18}O$ of MIPAS data were provided by Jonkheid et al. [8] for 1st of July, 2003. The MIPAS latitudinal distribution of $^{16}O^{16}O^{18}O$ shows a peak around 30–35 km for latitudes 90°N–50°S, but the ACE-FTS latitudinal distribution of $^{16}O^{16}O^{18}O$ does not show such a peak. The MIPAS latitudinal distribution [8] of $^{16}O^{18}O^{16}O$ does not show any features that appear in the ACE-FTS latitudinal distribution.

The mission average latitudinal distribution of the isotopologue $^{16}O^{17}O^{16}O$ shows a high fractionation (∼15%) band in the latitudes 27.5–30.5 km. It should be noted that the δ value standard deviations for the $^{16}O^{17}O^{16}O$ latitudinal distribution (Fig. 3e) were relatively high. Nevertheless, similar to the latitude distributions of $^{16}O^{18}O^{16}O$ (Fig. 2e) and $^{16}O^{16}O^{18}O$ (Fig. 1e), the latitude distribution of $^{16}O^{17}O^{16}O$ also shows higher fractionation where more sunlight is available (high values in the Northern Hemisphere during JJA and in Southern Hemisphere during DJF).

Standard deviations of all the isotopologues are more than 1 below 20.5 km (down to 6.5 km). Therefore the fractionations below 20.5 km in altitude were not considered in this study. There is a band of high fractionation values above 41.5 km for all the latitudinal distributions (>0.2 for $^{16}O^{16}O^{18}O$, >0.15 for $^{16}O^{18}O^{16}O$, >0.25 for $^{16}O^{17}O^{16}O$). The standard deviation of the observations are also increasing and this band may be an artifact; we have not considered these data. It is also possible that these high fractionation values are due to photolysis in the Hartley bands of ozone (e.g., [21]).

For comparison with the heavy ozone isotopologues, the parent ozone molecule was analyzed in the same way and the VMR distributions are presented in Fig. 5.

The ACE-FTS mission average altitude profiles of δ values $^{16}O^{16}O^{18}O$, $^{16}O^{18}O^{16}O$ and $^{16}O^{17}O^{16}O$ for 6 latitude bins were presented in the Figs. 6–8. Northern polar (90°N–60°N), northern mid-latitudes (60°N–30°N), southern tropics (30°S–0°S), northern tropics (0°N–30°N), southern mid-latitudes (30°S–60°S) and southern polar (60°S–90°S) are the 6 latitude regions that were considered in the analysis.

The ACE-FTS average altitude profiles of δ values of $^{16}O^{16}O^{18}O$ (Fig. 6) show a local minimum around 35 - 40 km in every latitude region. Typical fractionation values are 13–15% in the mid-stratosphere.

The ACE-FTS average altitude profiles of $^{16}O^{18}O^{16}O$ (Fig. 7) have typical δ values of about 10% in the mid stratosphere and increase above 35 km. The δ values are relatively constant in the tropics but increase with altitude at high latitudes.

δ values of the average altitude profiles of $^{16}O^{17}O^{16}O$ (Fig. 8) generally show a local minimum (8%) around 25 km and a local maximum (13%) around 29 km. These observations do not agree, for example, with the predicitions of Liang et al. [20] which have an increasing VMR with altitude.

The δ value profiles of $^{16}O^{16}O^{18}O$ and $^{16}O^{18}O^{16}O$ compared with MIPAS-Balloon measurements of Piccolo et al. [26] and FTIR profiles of Haverd et al. [16]. MIPAS-Balloon measurements were

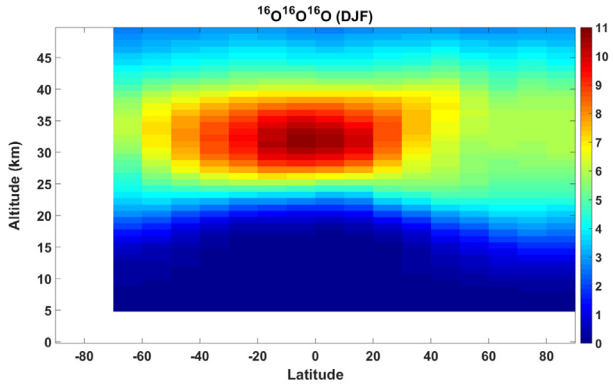

(a) $^{16}O^{16}O^{16}O$ (ppm) JJA

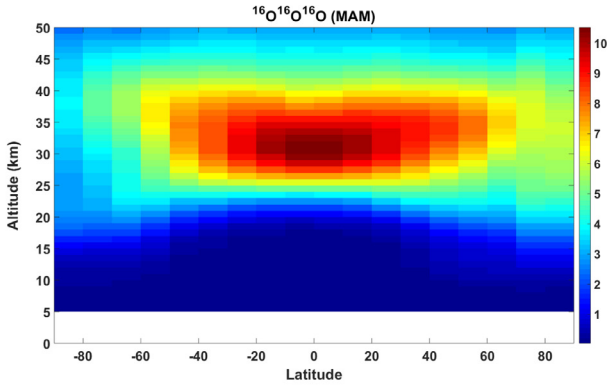

(b) $^{16}O^{16}O^{16}O$ (ppm) SON

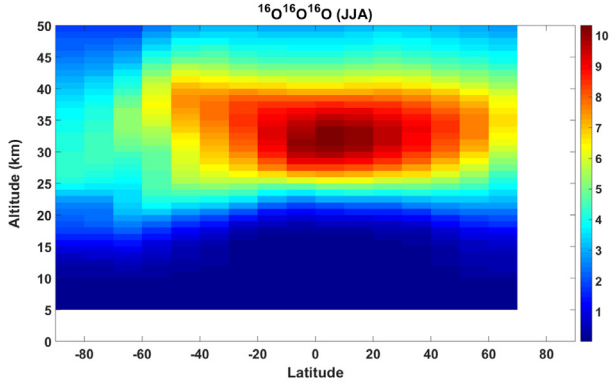

(c) $^{16}O^{16}O^{16}O$ (ppm) JJA

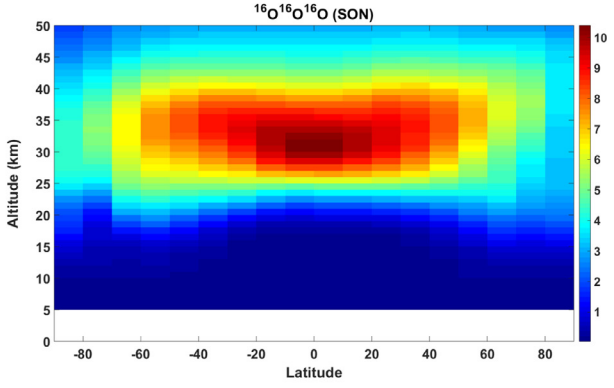

(d) $^{16}O^{16}O^{16}O$ (ppm) SON

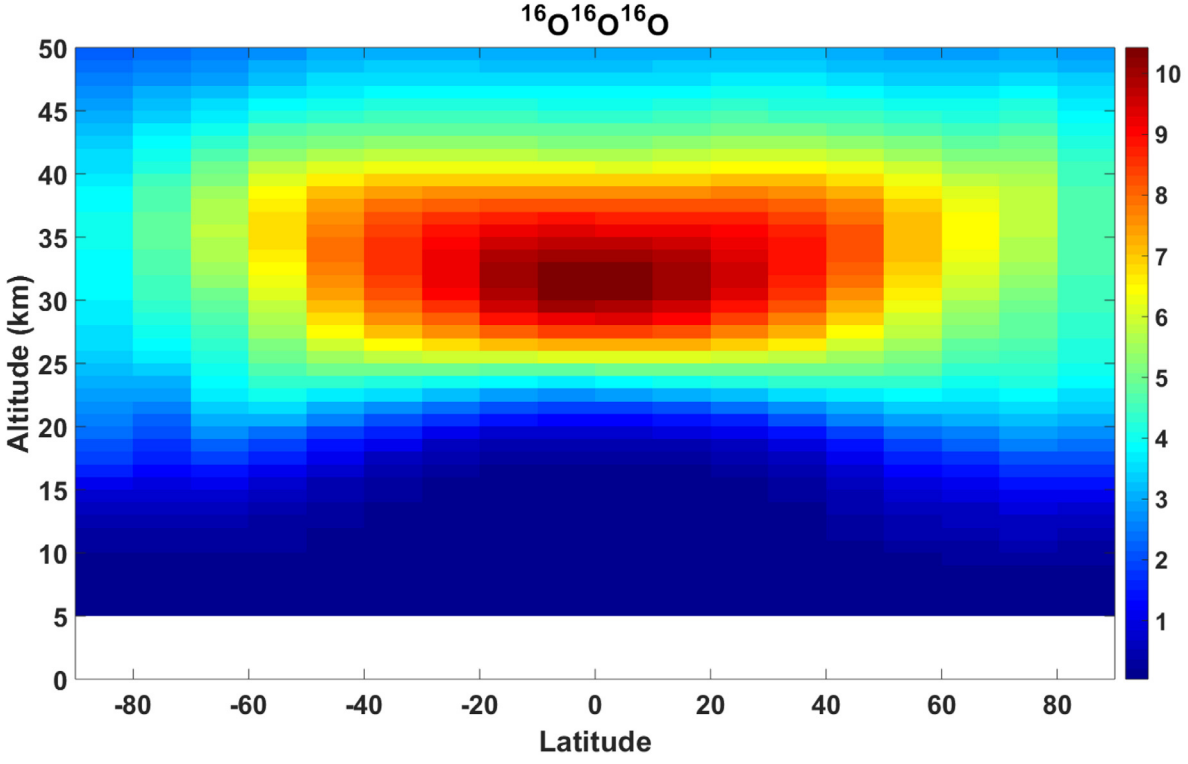

(e) $^{16}O^{16}O^{16}O$ mission average (ppm)

Fig. 5. $^{16}O^{16}O^{16}O$ VMRs in ppm

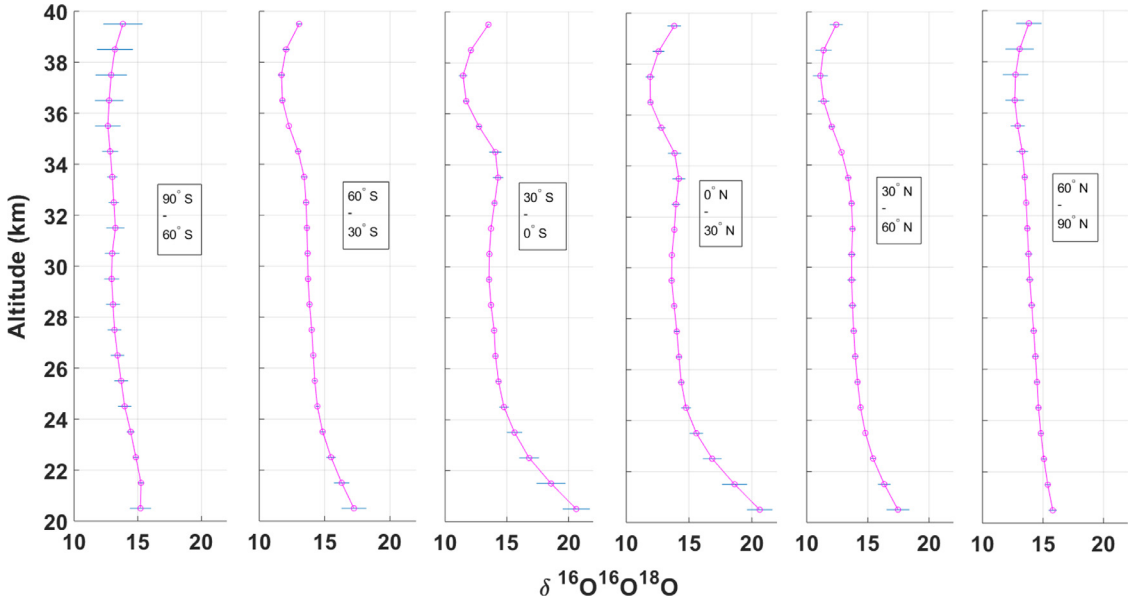

Fig. 6. Altitude profiles of δ% values of $^{16}O^{16}O^{18}O$ for different latitude bins

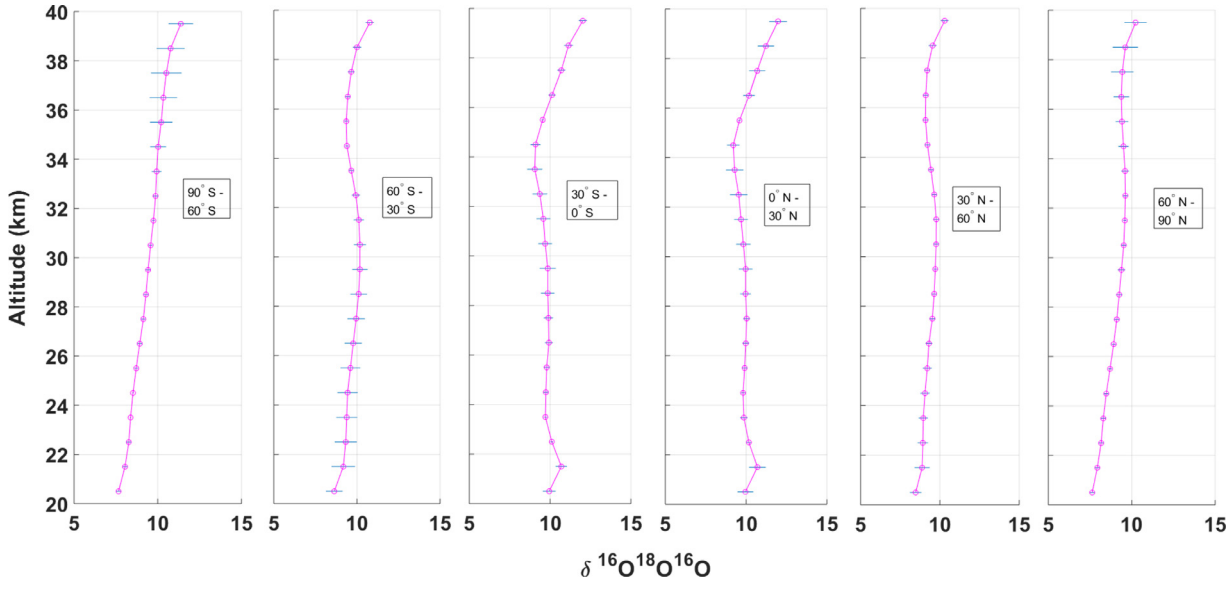

Fig. 7. Altitude profiles of δ% values of $^{16}O^{18}O^{16}O$ for different latitude bins

taken in Aire-sur-l'Adour, France (43.7°N) and in Kiruna, Sweden (67.5°N); and MkIV FTIR data in Fort Sumner (35°N) and in Fairbanks (65°N). There are several altitude profiles of δ values of $^{16}O^{16}O^{18}O$ and $^{16}O^{18}O^{16}O$ provided in Haverd et al. [16] that were obtained at Fort Sumner and Fairbanks. In order to compare these profiles with ACE-FTS data, two altitude profiles were selected that represent maximum and minimum δ values of Fort Sumner and Fairbanks profiles (Since δ value of $^{16}O^{18}O^{16}O$ profiles obtained at Fairbanks do not show much deviation from each other only one profile was selected). The ACE-FTS δ value profiles were obtained in the latitude regions 30°N–50°N and 60°N–70°N for comparison purposes (Fig. 9).

The ACE-FTS profile of $^{16}O^{16}O^{18}O$ in the region 30°N–50°N lies between the two altitude profiles obtained at Fort Sumner that were selected and within the error bars of the MIPAS-Balloon flight profile obtained at Aire-sur-l'Adour, France (43.7°N). The ACE-FTS profile of $^{16}O^{18}O^{16}O$ in the region 30°N–50°N generally agrees with the altitude profile of Haverd et al. [16] and lies slightly outside the error bars of the MIPAS-Balloon flight profile obtained at Aire-sur-l'Adour, France (43.7°N) (Fig. 9). The MIPAS-Balloon flight profile obtained at Kiruna, Sweden (67.5°N) of $^{16}O^{16}O^{18}O$ and $^{16}O^{18}O^{16}O$ are available only up to ~25 km. Both ACE-FTS $^{16}O^{16}O^{18}O$ and $^{16}O^{18}O^{16}O$ δ value profiles between 20.5 km and 25.5 km lie within the error bars of MIPAS-Balloon flight profile obtained at Kiruna, Sweden.

δ $^{50}O_3$ values reported in the Fig. 10 were obtained by using δ values calculated from $^{16}O^{18}O^{16}O$ and δ $^{16}O^{16}O^{18}O$ VMRs with the equation $\delta\ ^{50}O_3 = (2 \times \delta\ ^{16}O^{16}O^{18}O + \delta\ ^{16}O^{18}O^{16}O)/3$ in order to compare with mass spectrometric measurements. The ACE-FTS altitude profiles of δ $^{50}O_3$ values were calculated for 5 latitude regions. The ACE-FTS mission δ average altitude profiles of $^{50}O_3$ of 5 latitude regions were presented in the Figs. 10.

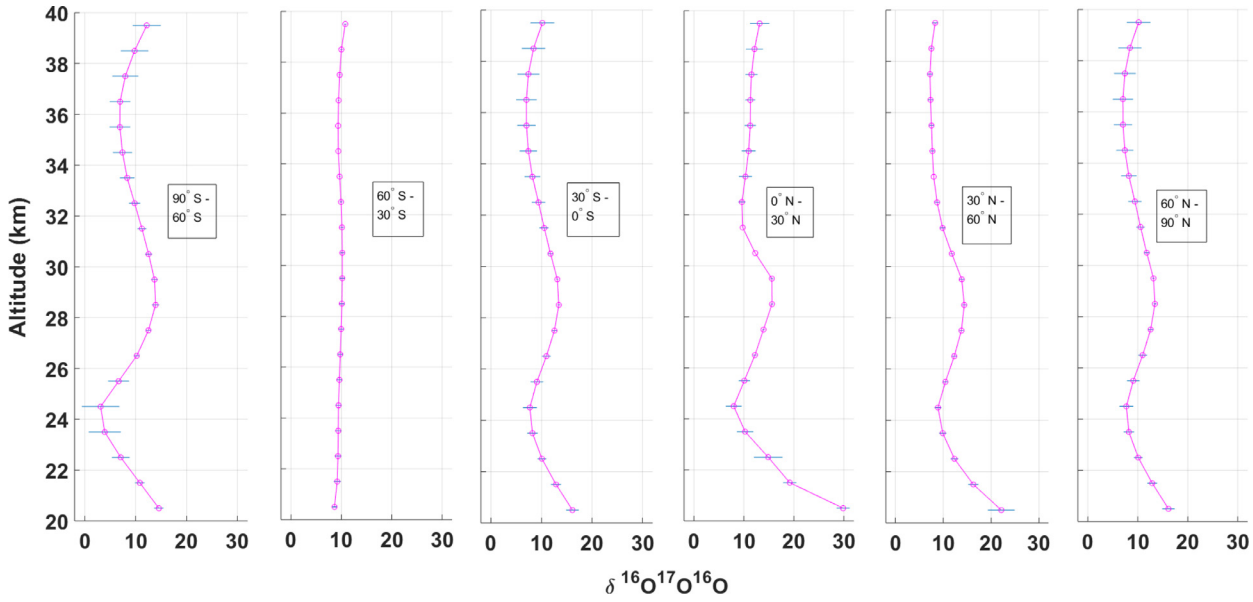

Fig. 8. Altitude profiles of δ% values of $^{16}O^{17}O^{16}O$ for different latitude bins

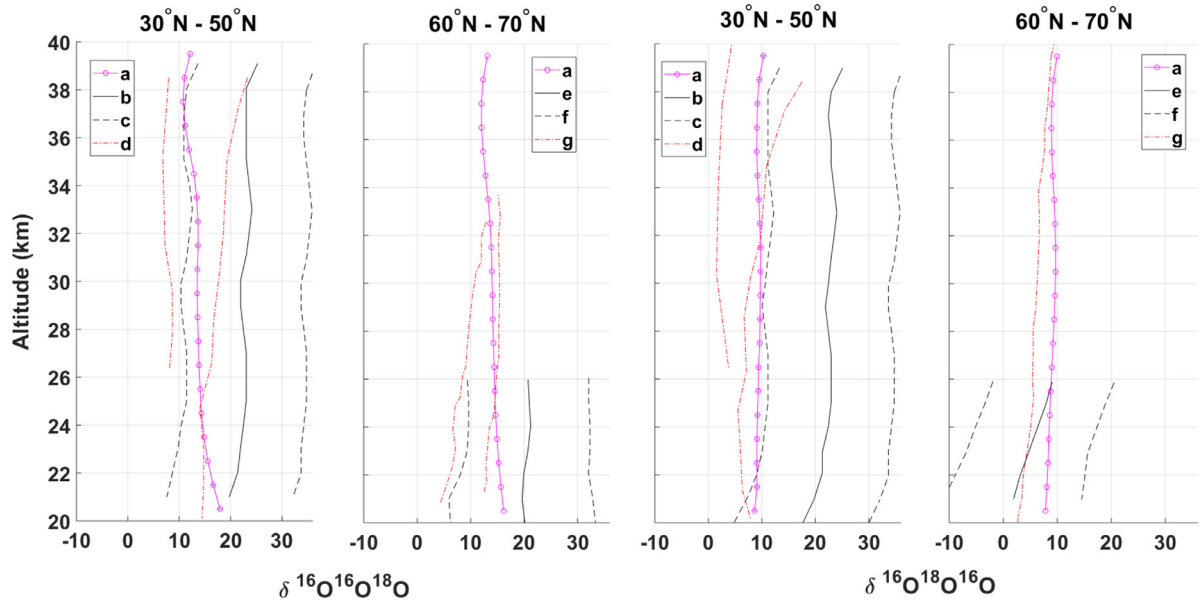

Fig. 9. Comparison of altitude profiles of δ% values of ozone isotopologues. (a) This study, (b) MIPAS-Balloon measurements at 43.7°N on September 2002 [26], (c) Uncertainty of MIPAS-Balloon measurements at 43.7°N for September 2002 [26], (d) MkIV FTIR data from Fort Sumner (35°N) flights [16], (e) Balloon-borne MIPAS-Balloon measurements at 67.5°N in March 2003 [26], (f) Uncertainty of MIPAS-Balloon measurements at 67.5°N for March 2003 [26], (g) MkIV FTIR data from Fairbanks (65°N) flights [16]

Southern polar (90°S–60°S), Southern mid-latitudes (60°S–30°S), tropics (30°S–30°N), northern mid-latitudes (30°N–60°N) and northern polar (60°N–90°N) are the 5 latitude regions considered in this analysis. The FIRS measurements are in the far infrared and the line parameters for these rotational transitions may be more reliable than the vibration-rotation line parameters used by the other remote sensing instruments. This type of systematic error has not been included in the quoted error bars. Overall, however, there is good agreement between ACE-FTS values and those of other instruments (Fig. 10).

Liang et al. [20] provide predictions of altitude dependent fractionation from their 1-dimentional semi-empirical model. As observed by ACE-FTS and predicted by Liang et al. [20] the fractionation of the symmetric isotopomers is substantially less than the asymmetric isotopomers. However, Liang et al. [20] predict that fractionation increases with altitude from 20 km to a peak near 35 km for all isotopologues. ACE-FTS altitude profiles vary with latitude but tend to be relatively flat (except for $^{16}O^{17}O^{16}O$) with an increase in fractionation near the top of the observed range above 35 km.

4. Conclusions

The ACE mission has an large ozone isotopologue data set for comparison with atmospheric chemical transport models that include isotopic fractionation. The fractionation with altitude is in

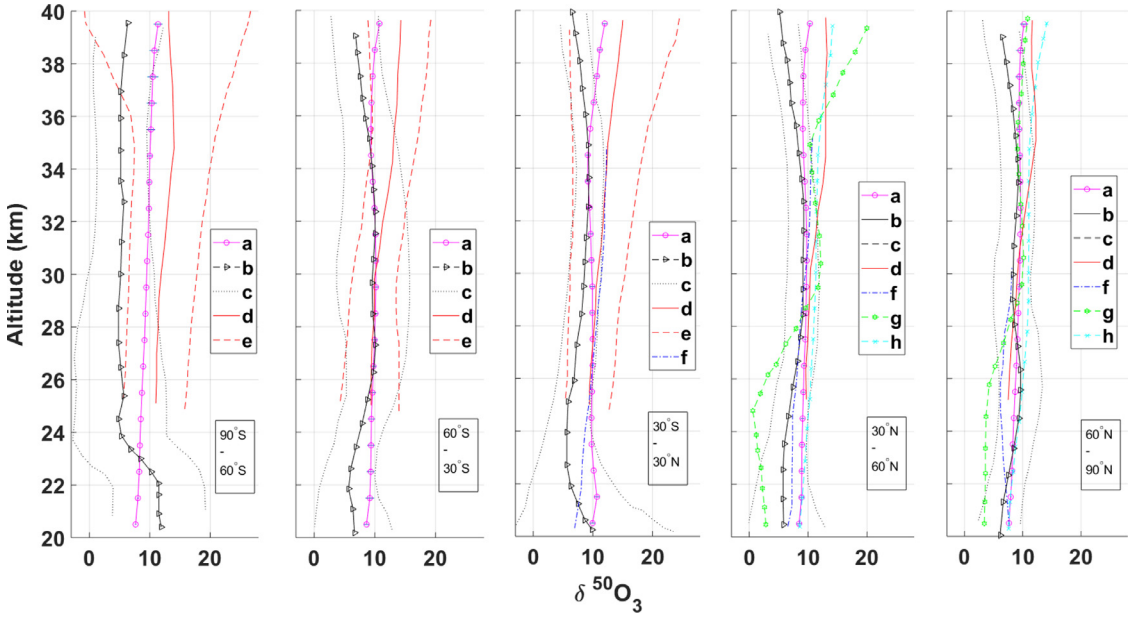

Fig. 10. Comparison of altitude profiles of δ% values of $^{50}O_3$. (a) This study, (b) MIPAS data of Jonkheid et al. [8], (c) Uncertainty in MIPAS data [8], (d) ATMOS IR measurements [7], (e) Uncertainty in ATMOS data [7], (f) Mass spectrometer data of Krankowsky et al. [5], (g) FIRS-2 measurements [6], (h) MkIV FTIR data [16]

general agreement with previous observations, although these observations are quite variable and often do not include error bars. Global distributions of isotopic ozone fractionations are observed for the first time. As expected the largest enrichments are observed in the tropical stratosphere in agreement with ballon-borne measurements. The contribution of photolysis to this fractionation can be seen in the tropics and at high latitudes in the summer. The upper stratosphere of the Antarctic polar vortex also shows enhanced fractionation possibly due to dynamics from descent of air enriched in heavy isotopologues.

Acknowledgement

The ACE mission is funded primarily by the Canadian Space Agency (CSA; 9F045-180032/001/MTB SCISAT).

Supplementary material

Supplementary material associated with this article can be found, in the online version, at doi:10.1016/j.jqsrt.2019.06.026.

References

[1] Cicerone RJ, McCrumb JL. Photodissociation of isotopically heavy O_2 as a source of atmospheric O_3. Geophys Res Lett 1980;7(4):251–4.
[2] Mauersberger K. Measurement of heavy ozone in the stratosphere. Geophys Res Lett 1981;8(8):935–7.
[3] Mauersberger K, Lämmerzahl P, Krankowsky D. Stratospheric ozone isotope enrichments revisited. Geophys Res Lett 2001;28(16):3155–8.
[4] Krankowsky D, Lämmerzahl P, Mauersberger K. Isotopic measurements of stratospheric ozone. Geophys Res Lett 2000;27(17):2593–5.
[5] Krankowsky D, Lämmerzahl P, Mauersberger K, Janssen C, Tuzson B, Röckmann T. Stratospheric ozone isotope fractionations derived from collected samples. J Geophys Res 2007;112(D8):D08301.
[6] Johnson DG, Jucks KW, Traub WA, Chance KV. Isotopic composition of stratospheric ozone. J Geophys Res 2000;105(D7):9025–31.
[7] Irion FW, Gunson MR, Rinsland CP, Yung YL, Abrams MC, Chang AY, et al. Heavy ozone enrichments from atmos infrared solar spectra. Geophys Res Lett 1986;23(17):2377–80.
[8] Jonkheid B, Röckmann T, Glatthor N, Janssen C, Stiller G, von Clarmann T. Retrievals of heavy ozone with MIPAS. Atmos Measur Tech 2016;9(12):6069–79.
[9] Mauersberger K, Erbacher B, Krankowsky D, Günther J, Nickel R. Ozone isotope enrichment: isotopomer-specific rate coefficients. Science 1999;283(5400):370–2.
[10] Janssen C, Guenther J, Krankowsky D, Mauersberger K. Temperature dependence of ozone rate coefficients and isotopologue fractionation in ^{16}O - ^{18}O oxygen mixtures. Chem Phys Lett 2003;367(1):34–8.
[11] Thiemens MH, Heidenreich JE. The mass-independent fractionation of oxygen: a novel isotope effect and its possible cosmochemical implications. Science 1983;219(4588):1073–5.
[12] Schinke R, Grebenshchikov SY, Ivanov M, Fleurat-Lessard P. Dynamical studies of the ozone isotope effect: astatus report. Ann Rev Phys Chem 2006;57(1):625–61.
[13] Brenninkmeijer CAM, Janssen C, Kaiser J, Röckmann T, Rhee TS, Assonov SS. Isotope effects in the chemistry of atmospheric trace compounds. Chem Rev 2003;103(12):5125–62.
[14] Gao YQ, Marcus RA. Strange and unconventional isotope effects in ozone formation. Science 2001;293:259–63.
[15] Gao YQ, Marcus RA. An approximate theory of the ozone isotopic effects: rate constant ratios and pressure dependence. J Chem Phys 2007;127(24):244316.
[16] Haverd V, Toon GC, Griffith DWT. Evidence for altitude-dependent photolysis-induced ^{18}O isotopic fractionation in stratospheric ozone. Geophys Res Lett 2005;32(22).
[17] Chakraborty S, Bhattacharya SK. Oxygen isotopic fractionation during uv and visible light photodissociation of ozone. J Chem Phys 2003;118(5):2164–2172.
[18] Cole AS, Boering KA. Mass-dependent and non-mass-dependent isotope effects in ozone photolysis: resolving theory and experiments. J Chem Phys 2006;125(18):184301.
[19] Miller CE, Onorato RM, Liang M-C, Yung YL. Extraordinary isotopic fractionation in ozone photolysis. Geophys Res Lett 2005;32(14).
[20] Liang M-C, Blake GA, Yung YL. A semianalytic model for photo-induced isotopic fractionation in simple molecules. J Geophys Res 2004;109(D10):D02302.
[21] Ndengué S, Madronich S, Gatti F, Meyer H-D, Motapon O, Jost R. Ozone photolysis: strong isotopologue/isotopomer selectivity in the stratosphere. J Geophys Res 2014;119(7):4286–302.
[22] Früchtl M, Janssen C, Taraborrelli D, Gromov S, Röckmann T. Wavelength-dependent isotope fractionation in visible light O_3 photolysis and atmospheric implications. Geophys Res Lett 2015;42(20):8711–18.
[23] Früchtl M, Janssen C, Röckmann T. Experimental study on isotope fractionation effects in visible photolysis of O_3 and in the O + O_3 odd oxygen sink reaction. J Geophys Res 2015;120(9):4398–416.
[24] Bernath P. The atmospheric chemistry experiment (ACE). J Quant Spectrosc Radiat Transf 2017;186:3–16.
[25] Rothman L, Jacquemart D, Barbe A, Benner DC, Birk M, Brown L, et al. The HITRAN 2004 molecular spectroscopic database. J Quant Spectrosc Radiat Transf 2005;96(2):139–204.
[26] Piccolo C, Dudhia A, Payne VH. Heavy ozone enrichments from MIPAS limb emission spectra. Atmos Chem Phys Discuss 2009;9:25127–58.
[27] Slater C, Preston T, Weaver LT. Stable isotopes and the international system of units. Rapid Commun Mass Spectr 2001;15(15):1270–3.